

Innovative approach of in-situ fixed mode dual effect (photo-Fenton and photocatalysis) for ofloxacin degradation

Kritika Sharma*, Steffi Talwar**, Anoop Kumar Verma***,†, Diptiman Choudhury*, and Borhan Mansouri****

*School of Chemistry and Biochemistry, Thapar Institute of Engineering and Technology, Patiala, India

**Department of Chemical Engineering, Thapar Institute of Engineering and Technology, Patiala, India

***School of Energy and Environment, Thapar Institute of Engineering and Technology, Patiala, India

****Substance Abuse Prevention Research Center, Health Institute, Kermanshah University of Medical Sciences, Kermanshah, Iran

(Received 4 July 2019 • accepted 12 November 2019)

Abstract—Novel composite materials composed of clay, foundry sand (FS), and fly-ash (FA) have been employed to immobilize TiO₂ for incorporating in-situ dual effect for the degradation of antibiotic ofloxacin. The in-situ generation of iron from the composite beads with surface active TiO₂ induced the dual effect of photo-Fenton and photocatalysis. FA/FS/TiO₂ beads illustrated the best results (92% removal) at optimized conditions in the batch reactor experiments. The increment in the rate constant along with a decrease in treatment time for the dual effect has proven the credentials of the in-situ dual effect. Synergy in first-order rate constant using dual process was 51% over the single processes of photo-Fenton and photocatalysis. After 35 recycles the viability of the composed beads was observed through SEM/EDS, UV-DRS and FT-IR analysis, which further justified its use industrially. Estimation of nitrate, nitrite, and ammonia as its by-products was performed for the confirmation of mineralization. Generation of the intermediate products was also identified through GC-MS analysis, and a degradation pathway was proposed. Toxicity test confirming the nontoxic nature of the treated solution was performed on *E. coli* grown in Miller's Luria Bertani Broth nutrient medium.

Keywords: Ofloxacin, In-situ Dual Effect, Composite Beads, Synergistic Effect

INTRODUCTION

The pharmaceutical segment of India represents 10% of the worldwide pharmaceutical industry in terms of volume and 3.1-3.6% in terms of value [1]. Easy availability of pharmaceutical drugs, and subsequent over usage, has led to an increase in the concentration of drugs in water sources in resulting in the antimicrobial resistance [2]. Moreover, the wastewater released from the pharmaceutical industries carries chemicals and untreated by-products along with it. Therefore, this wastewater requires prior treatment to remove these compounds prior to its discharge into the environment [3]. The presence of these types of contaminants in surface water and fresh water confirms the inability of conventional methods, as these are not sufficient to eradicate bio-recalcitrant industrial wastes so far [4,5].

Literature in the recent past has shown the capability of the advanced oxidation process (AOP) employed for the treatment of dyes, textiles, pharmaceuticals and other industrial effluents. AOPs include homogeneous processes such as ozonation, photolysis, photo-Fenton, UV/H₂O₂ [6,7] and heterogeneous including photocatalysis [8,9]. The basic process of AOP involves the oxidation of pollutant using hydroxyl radicals ([•]OH). Among the wide range of AOP processes, fixed bed heterogeneous and homogeneous photocatalysis have shown its credentials towards field-scale applications as

compared to other processes [10]. The catalyst is immobilized over the fixed-bed surface, which helps in overcoming the limitation of catalyst separation [11-13], whereas the homogeneous system (photo-Fenton) deals with a system having good potential of scale-up. However, shortcomings like electron-hole pair recombination, iron sludge formation, mass transfer limitations and increase in treatment time really pose a threat for visualization of their field-scale applications.

Hence, keeping in mind the virtues and shortcomings of the above-mentioned processes, the combination of these processes via in-situ approach seems to be a novel concept. Here, the concept of a composite material made up of fly ash (FA) and foundry sand (FS) has been proposed with a surface coating of TiO₂. Along with continuous leaching of iron (from FS and FA) and with the catalyst fixation on its surface, in-situ dual effect (photo-Fenton and photocatalysis) raises the degradation quotient many times. Research in this specific zone has been continually engaged towards decreasing the time for the removal of drug along with an intensification in the rate of reaction. In this investigation, the novel idea of inducing the dual effect of photocatalysis and photo-Fenton is proposed in the context of decreasing treatment time for the removal of ofloxacin. This technique has tremendous effectiveness in terms of degradation, however, not much applied well yet.

The enhanced degradation by the dual process can be ascribed to the creation of an adequate measure of hydroxyl radicals produced at the same time by both continuous procedures. Additionally, iron decreases the coupling of electron-holes in TiO₂, hence upgrading its photocatalytic action. The capability of waste materials (FS and FA) that could be reused and utilized as a cost-effective

†To whom correspondence should be addressed.

E-mail: anoop.kumar@thapar.edu

Copyright by The Korean Institute of Chemical Engineers.

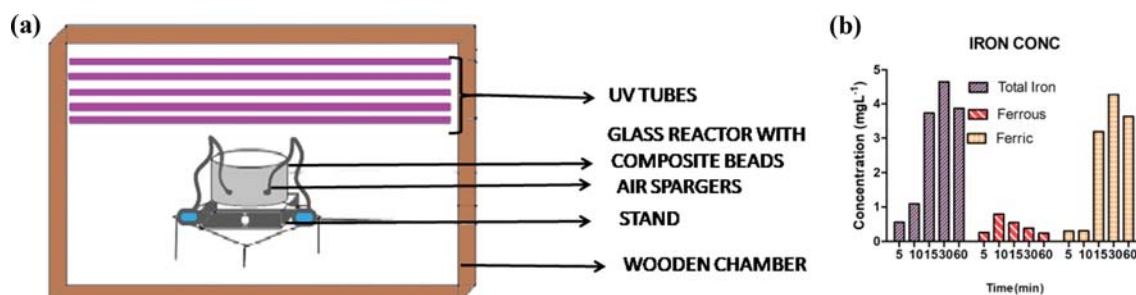


Fig. 1 (a) A line diagram of the experimental setup for conducting dual effect experiments, (b) the concentration of total, Fe (II), and Fe (III) ions with the passage of time during the degradation of ofloxacin.

iron source in the process has been proposed, which is a new process. The basic mechanism of the dual process is the generation/leaching of Fe (II) and Fe (III) ions in the solution [14]. The Fe (II) ions are engaged in photo-Fenton reactions along with H_2O_2 and light. The TiO_2 coating on the surface of the beads leads to the photocatalytic process. The operational problem of electron and hole recombination could be avoided by using this electron to interact with Fe (III) ions. Hence, the Fe (III) ions leached from the beads combine with the electrons to form Fe (II), which is again used in the photo-Fenton process to continue. Thus this dual impact has the prompt synergistic impact of both the processes at the same time and the same place, leading to the faster removal of the compounds.

In the current study, the degradation studies of the pharmaceutical compound, ofloxacin have been discussed using in-situ dual effect. Ofloxacin being a synthetic broad-spectrum antibacterial drug administered orally is a fluorinated carboxyquinolone. Mostly 80% of the fluoroquinolones are excreted, as it is in its active form. This lead to its increased concentrations in the sewage and ultimately to the fresh and surface water. High ofloxacin concentrations have been identified in municipal wastewater treatment plant effluent ($53\text{--}1,800\text{ ng L}^{-1}$), surface water ($10\text{--}535\text{ ng L}^{-1}$), hospital wastewater ($25,000\text{--}35,000\text{ ng L}^{-1}$) confirming the inability of the conventional treatment process [15,16]. Ofloxacin was used as the target pollutant for the research work. Hence in this study, novel support material composed of industrial waste products FS and FA as an elective iron source along with an immobilized layer of TiO_2 has proven to be a very effective treatment for such chemical containing wastewater.

METHODS AND MATERIALS

Ofloxacin, a synthetic antibacterial drug administered orally, was obtained from the nearby pharmaceutical industry in Patiala, Punjab, India. Photocatalyst, $P25\text{-}TiO_2$, was purchased from Evonik Industries (India). The oxidant used for the reaction, Hydrogen peroxide (H_2O_2 (30% w/v)) was procured from Ranbaxy (India). Clay was bought from a local vendor, while fly ash (FA) and waste foundry sand (FS) were accepted from a local industry, Patiala, Punjab (India) as gift samples for the preparation of inert fixed-bed materials and were utilized without any further purification. Acetic acid (>99.5%) and sodium acetate (>98.5%) for the acetate buffer were obtained from TCI Chemicals (India) Pvt. Ltd. For all the

reactions and for the preparation of all reagents double distilled water was used.

1. Experimental Set-up and Procedure

For carrying out the experiments, a wooden chamber with UV tubes ($36\text{ W}\times 7$, $\lambda=365\text{ nm}$ (UV-A, Philips)) fitted at the top was used (Fig. 1(a)). A borosilicate glass batch reactor (1,200 mL) was used for lab scale experiments with a height of 5.2 cm and diameter of 17.4 cm. Aeration was provided by using spargers with an average flow rate of 3 L min^{-1} . Clay was used as binding material for composing the beads. Spherical beads were formulated manually by taking accurate proportions of the clay, FS and FS (2:1:1, respectively). The beads were solidified by heating in the muffle at $1,000\text{ }^\circ\text{C}$ for 3 h and then cured in water for gaining the proper strength. The beads were immobilized using TiO_2 by the standard dip-coating method [17]. For the accomplishment of dual effect reactions, the TiO_2 coated composite beads were dipped inside the working solution of ofloxacin ($C_0=25\text{ mg L}^{-1}$) with maintained pH of 3.5 and 300 mg L^{-1} of H_2O_2 addition. After uniform intervals of time, the required amount of sample was withdrawn and subsequently analyzed for degradation. The Fe (II) and Fe (III) concentration was determined at various intervals during the course of the reaction (Fig. 1(b)). For executing the dual effect experiments, the pH was set at acidic conditions due to the better leaching of iron required for the photo-Fenton studies.

1-1. Bioassay Test

A bioassay test for the untreated and treated ofloxacin solution was conducted by using *E. coli* DH-5 α strain. For this study, *E. coli* was grown in Miller's Luria Bertani Broth (LB) (Tryptone 10 g L^{-1} , Yeast extract 5 g L^{-1} , Sodium chloride 10 g L^{-1}) in double-distilled water. The test was performed by the zone inhibition method, which is also termed as the Kirby-Bauer method. The bacterial culture with various concentrations of ofloxacin in the agar plate was cultured for 24 hours in the incubator at $37\text{ }^\circ\text{C}$.

2. Chemical Analysis and Characterization Techniques

Sample analysis was done using UV-Vis spectrophotometer (LABINDIA, T60 U, India). For the estimation of iron (Total, Ferrous, and Ferric), nitrite ions, nitrate ions, and COD standard APHA methods were used [18]. SEM (JSM-6510LV, JEOL, Japan) and EDS (INCAX-act, Oxford Instruments, United Kingdom) analysis were used for determining the morphology and elemental composition of the coated and uncoated composite support beads. UV-DRS (UV-2600, Shimadzu (Asia pacific)) was used for the evaluation of band gap energy. It was recorded by using $BaSO_4$ as the reference.

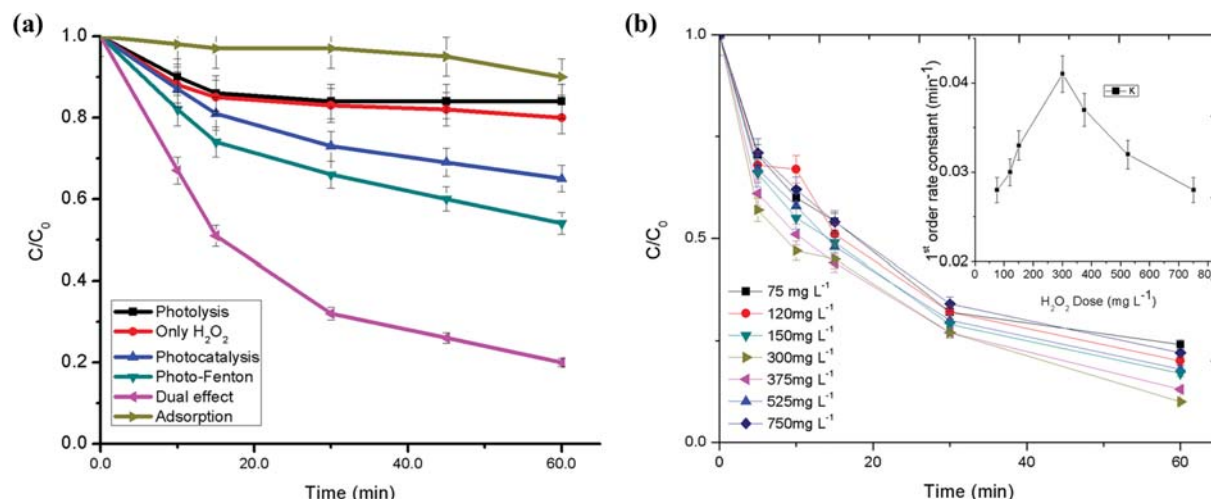


Fig. 2 (a) Comparison of different processes for the degradation of ofloxacin, (b) plot of first-order rate constant for the effect of a change in H_2O_2 dose, effect of the dose of H_2O_2 on the degradation of ofloxacin using C/C_0 vs time graph ($C_0=25 \text{ mg L}^{-1}$, $\text{pH}=3.5$, A/V ratio of $0.273 \text{ cm}^2 \text{ mL}^{-1}$) (inset).

Fourier transform infrared spectroscopy, Perkin Elmer, RX1 was used for the evaluation of functionalized groups, linkages and bonding of compounds in the prepared catalyst and was performed in the range of $4,000\text{--}200 \text{ cm}^{-1}$ using KBr pellets. GC-MS as well as LCMS analysis of ofloxacin was performed to recognize the organics transformation products and various intermediates. Transformation products of ofloxacin were analyzed by ultra-performance liquid chromatography coupled with mass spectrometry, using UPLC-XEVO-G2-XS/QTOF-MS (Waters) equipped with C18 column (100×2.1 ; $1.7 \mu\text{m}$). The mobile phase was comprised of 0.1% formic acid in water and acetonitrile. Other operating parameters were as follows: source temperature, $120 \text{ }^\circ\text{C}$; desolvation temperature, $350 \text{ }^\circ\text{C}$; carrier gas, N_2 ; cone gas flow, 60 L h^{-1} . Perkin-Elmer Clarus 500 MS instrument was used for the GC-MS analysis with capillary columns made of fused silica ($25 \text{ m} \times 0.20 \mu\text{m}$ internal diameter) coated with a 95% Dimethyl Polysiloxane/5% diphenyl. Injector temperature of $300 \text{ }^\circ\text{C}$ was used for the split/splitless injector mode. Helium was used as a carrier gas with a flow rate of 1 mL min^{-1} . The temperature subsequent to the ion source and inlet line was set at 280 and $250 \text{ }^\circ\text{C}$, respectively, with sample run time of 26 min.

RESULTS AND DISCUSSION

1. Preliminary Studies

To confirm the tremendous dual effect on the degradation of the ofloxacin, various preliminary experiments were performed. When the ofloxacin solution was exposed to UV light, only 16% of degradation was observed after 1-h reaction in a batch reactor. The adsorption studies conducted in dark showed only 7% reduction of the compound after 1 h. When H_2O_2 alone was used, 19% of degradation was achieved, which might have been due to the production of hydroxyl radicals. While in one hour 45% degradation was observed using the photo-Fenton technique in which only the iron and hydroxyl radical production by H_2O_2 was responsible for the reduction in the concentration of the compound. The degradation of the compound using the photocatalytic process was

25% in one hour. Significant decline in the ofloxacin concentration was observed when the dual process (photo-Fenton+photocatalysis) was employed, and it showed about 80% degradation in only 1 h (Fig. 2(a)). Hence, these preliminary studies confirmed that the dual process is quite effective in the degradation of ofloxacin at a faster rate and in less time. Significant increase in the rate constant was also observed in case of dual effect as compared to individual processes as discussed in the subsequent sections.

The kinetic study of photocatalytic degradation of ofloxacin has been described using the first-order kinetic model.

$$\ln\left(\frac{C}{C_0}\right) = kt \quad (1)$$

where k is the first-order rate constant of the reaction (min^{-1}). C_0 is the initial concentration of ofloxacin, C is the final concentration (mg L^{-1}), t is the degradation time (min). As predicted, the value of the first-order rate constant for dual-process came out to be (0.031 min^{-1}) higher than the individual processes of photo-Fenton (0.01 min^{-1}) and photocatalysis (0.008 min^{-1}).

2. Effects of Various Parameters

2-1. Effect of the Oxidant Dosage

The oxidant dose plays an important role in both the processes, in photo-Fenton as well as in photocatalysis, since it prompts the production of hydroxyl radicals as soon as the electron gets excited by a photon of light to a higher energy state. It additionally produces $\cdot\text{OH}$ as per the following equation:



Thus the rate of reaction accelerates with the addition of the H_2O_2 . In this context, H_2O_2 concentration was varied in the range of 75 mg L^{-1} to 750 mg L^{-1} keeping the volume (200 mL) and pH (3.5) of the solution constant. Nearly 27% increment in the rate constant was observed in the degradation of ofloxacin when the concentration of the oxidant was increased up to 300 mg L^{-1} . Actually, H_2O_2 plays an important role in both the processes, in photocatalysis as well as in photo-Fenton, which is visualized in the in-

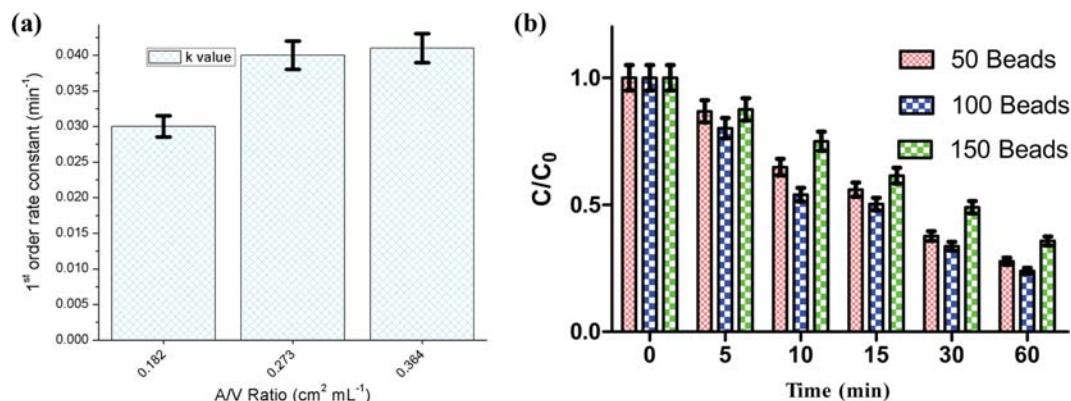


Fig. 3. (a) The plot of first-order rate constant for the effect of the change in A/V (at $C_0=25 \text{ mg L}^{-1}$, $\text{pH}=3.5$, H_2O_2 dosage of 300 mg L^{-1}), (b) effect of change in the covered surface area on the degradation of ofloxacin (at the optimized conditions of $C_0=25 \text{ mg L}^{-1}$, $\text{pH}=3.5$, H_2O_2 dosage of 300 mg L^{-1} , A/V ratio of $0.273 \text{ cm}^2 \text{ mL}^{-1}$).

creased value of the rate constant. But after further increment in the H_2O_2 concentration, the degradation rate becomes slower due to the excess oxidant causing scavenging effect [19]. Thus, from these variations, it was observed that the optimum amount of the oxidant would be 300 mg L^{-1} for the execution of the dual process as shown in Fig. 2(b).

2-2. Area/Volume Ratio Effect of the Batch Reactor

In the large-scale application of AOPs the depth of the reactor forms a major limitation, as the penetration of solar radiations should be sufficient to reach the solution containing pollutants. Generally, less depth and more exposed area are recommended for the better penetration of light. In our studies, this was achieved after varying the volume of the solution and keeping the area of the batch reactor constant. Although there are some studies reporting the A/V ratio effect, but the degradation of priority pollutants is more promising in case of dual effect [20]. In this context, the A/V ratio of the reactor was varied in the range of $0.182 \text{ cm}^2 \text{ mL}^{-1}$ to $0.364 \text{ cm}^2 \text{ mL}^{-1}$. With an increase in the A/V ratio from $0.182 \text{ cm}^2 \text{ mL}^{-1}$ to $0.273 \text{ cm}^2 \text{ mL}^{-1}$, the rate of degradation was increased by 27% as the penetration of light through the solution and reaching the beads surface increased. Better penetration of light would lead to the more hydroxyl radicals generation in the solution, thus subsequently intensifying the degradation rate. With further increase in the A/V ratio, there was not much increase in the degradation rate, thus keeping

the A/V ratio at $0.273 \text{ cm}^2 \text{ mL}^{-1}$ (Fig. 3(a)). This A/V ratio would really help in large scale applications of this technology in context to the area calculations.

2-3. Variation in the Number of Composite Beads

For visualization of field-scale applications of the proposed technology, the amount of catalyst required would be an important parameter to consider. In the present study, this parameter was covered by varying the number of catalyst coated beads. Actually, the covered surface area of the batch reactor (used in the study) varied with the variation of a number of beads, which subsequently affected the degradation rate. In this context, the coated beads varied in number from 50 to 150 of the total surface area available. It was detected that when the surface of the reactor was covered with 50 beads (i.e., almost 50% of the available surface area of batch reactor used), 71% of the degradation was obtained. If the reactor's surface was fully covered, i.e., 100% with almost 100 beads, maximum degradation of 92% was obtained owing to the appropriate amount of iron leached from the composite as well as significant amount of hydroxyl radical production leading to increase in the rate constant by 33%. But with further increase in a number of beads to 150, i.e., overlapping to 150%, the degradation rate was slowed by 24% as seen in Fig. 3(b). This might be due to the shadow effect: formation of the dead zones. With the increase in iron content and dose of TiO_2 , most of the active sites got blocked, which

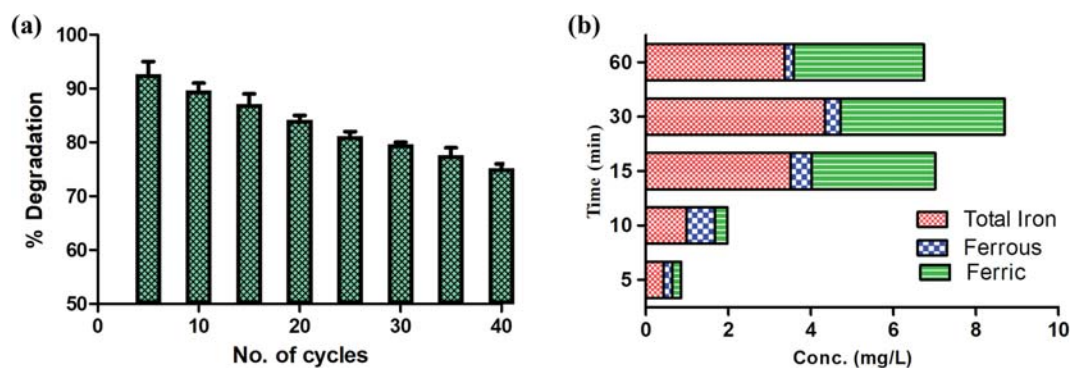


Fig. 4. (a) Durability of the TiO_2 coated composite beads, (b) total, Fe (III) and Fe (II) ion concentration leaching from the beads after 35 recycles.

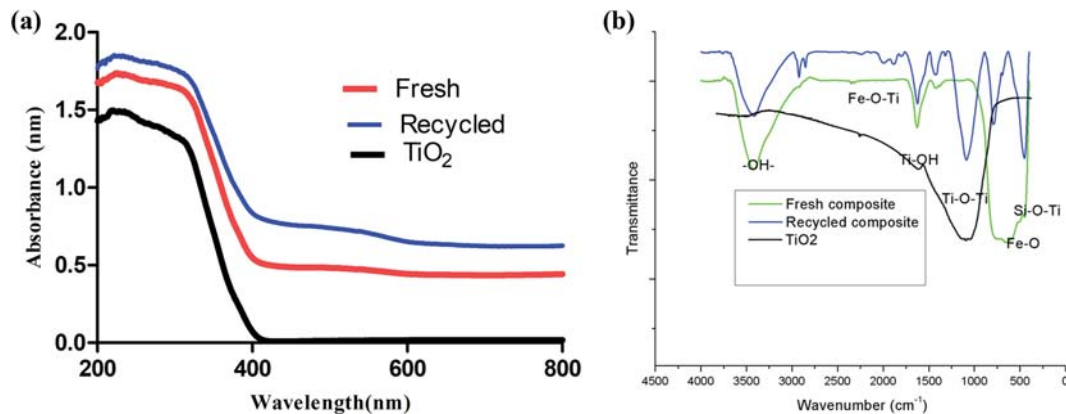


Fig. 5. (a) UV-Vis DRS for the pure TiO_2 catalyst, fresh and recycled composite beads, (b) FT-IR graph of the catalyst (TiO_2), freshly composite and recycled composite beads.

might have led to decreased degradation rate.

3. Durability Studies

For the large scale applications of the dual effect, durability of the supported catalyst plays an important role [10]. The implication of the process is to reuse the same composite beads for various recycles without actual loss in the activity. Being dual in nature, iron content leaching from the beads as well as the amount of TiO_2 coated on the surface of beads plays a major role. In the current study, it was observed that the immobilized TiO_2 and leached iron content from the composite beads were effectively durable enough even after thirty to forty cycles, as shown in Fig. 4. The gradual reduction in dual effect (10–12%) after thirty cycles may be ascribed to the loss of the catalyst and less amount of iron leaching into the solution during consecutive cycles of the reaction. The stability of the catalyst and iron presence in the beads was determined by SEM-EDS of the fresh beads, coated beads, and recycled immobilized beads; it was found that the catalyst was intact and iron was still actively leaching even after 35 cycles.

4. Synergistic Effect

During the degradation studies of pharmaceutical compound ofloxacin, it was observed that the synergistic effect [21] of the dual process over the photo-Fenton was 71.95%, while that on photocatalysis was 80%. The total synergy of dual process over both photocatalysis and photo-Fenton processes was calculated to be 51.9%.

The synergy calculations of the dual process over only photocatalysis process:

$$\begin{aligned} \% \text{ Synergy} &= 100 \times \{(k_{\text{dual}} - k_{\text{photocatalysis}}) / k_{\text{dual}}\} & (3) \\ \% \text{ Synergy} &= 100 \times \{(0.041 - 0.0082) / 0.041\} \\ \% \text{ Synergy} &= 80\% \end{aligned}$$

The synergy calculations of the dual process over only photo-Fenton process:

$$\begin{aligned} \% \text{ Synergy} &= 100 \times \{(k_{\text{dual}} - k_{\text{photoFenton}}) / k_{\text{dual}}\} & (4) \\ \% \text{ Synergy} &= 100 \times \{(0.041 - 0.0115) / 0.041\} \\ \% \text{ Synergy} &= 71.95\% \end{aligned}$$

The synergy calculations of the dual process over both photo-Fenton and photocatalysis process i.e overall synergy:

$$\begin{aligned} \% \text{ Synergy} &= 100 \times \{(k_{\text{dual}} - (k_{\text{photocatalysis}} + k_{\text{photoFenton}})) / k_{\text{dual}}\} & (5) \\ \% \text{ Synergy} &= 100 \times \{(0.041 - (0.0082 + 0.0115)) / 0.041\} \\ \% \text{ Synergy} &= 51.9\% \end{aligned}$$

Hence, the synergistic impact of the dual technique over both the individual processes led to the tremendous increment in the reaction rate of confirming the viability of the dual effect.

5. Characterization Analysis

5-1. UV-DRS Analysis

Band gap energy was evaluated using UV-Vis diffuse reflectance spectra [22]. A comparison was made between recycled Fe- TiO_2 composite and fresh TiO_2 P25 powder samples (Fig. 5(a)). The spectra obtained from Fe- TiO_2 composite sample displayed that due to the presence of iron in composite, the light was able to absorb in the visible region also. The band gap of the prepared catalyst and TiO_2 P25 was estimated by the equation:

$$E_g = h\nu = hc/\lambda \quad (6)$$

Here, E_g is the band gap energy (eV), c is the speed of light, h is the Planck constant and λ is the wavelength.

Utilizing the given equation, the value of band gap energy was 3.2 eV for P-25 TiO_2 , 3.18 eV for the fresh catalyst (beads) and 3.15 eV for the recycled catalyst (beads), confirming the activity of the catalyst even after repeated use and not much reduction in the band gap energy after reuse.

5-2. FT-IR Analysis

Fig. 5(b) shows the peaks confirming the presence of Ti-O-Ti bonds in the range 800–1,200 cm^{-1} [23] for both the fresh and recycled spectrum, which claims the presence of TiO_2 lattice in the composite beads. Strong peaks were obtained for Si-O-Ti. The initial stretching in the recycled as well as fresh composite was displayed the presence of Fe-O in the sample. The formation of Fe-O-Ti bond was confirmed by the broad peak appearing at 2,378.19 cm^{-1} in the spectra [24]. The O-H groups stretching vibrations were related with the occurrence of transmittance band at 3,407.91 cm^{-1} and 3,410.82 cm^{-1} in case of TiO_2 and composite beads.

5-3. SEM-EDS Analysis

Also, the scanning electron microscopy-energy dispersive X-ray spectroscopy images are depicted in Figs. 6(a), (b), (c). For the

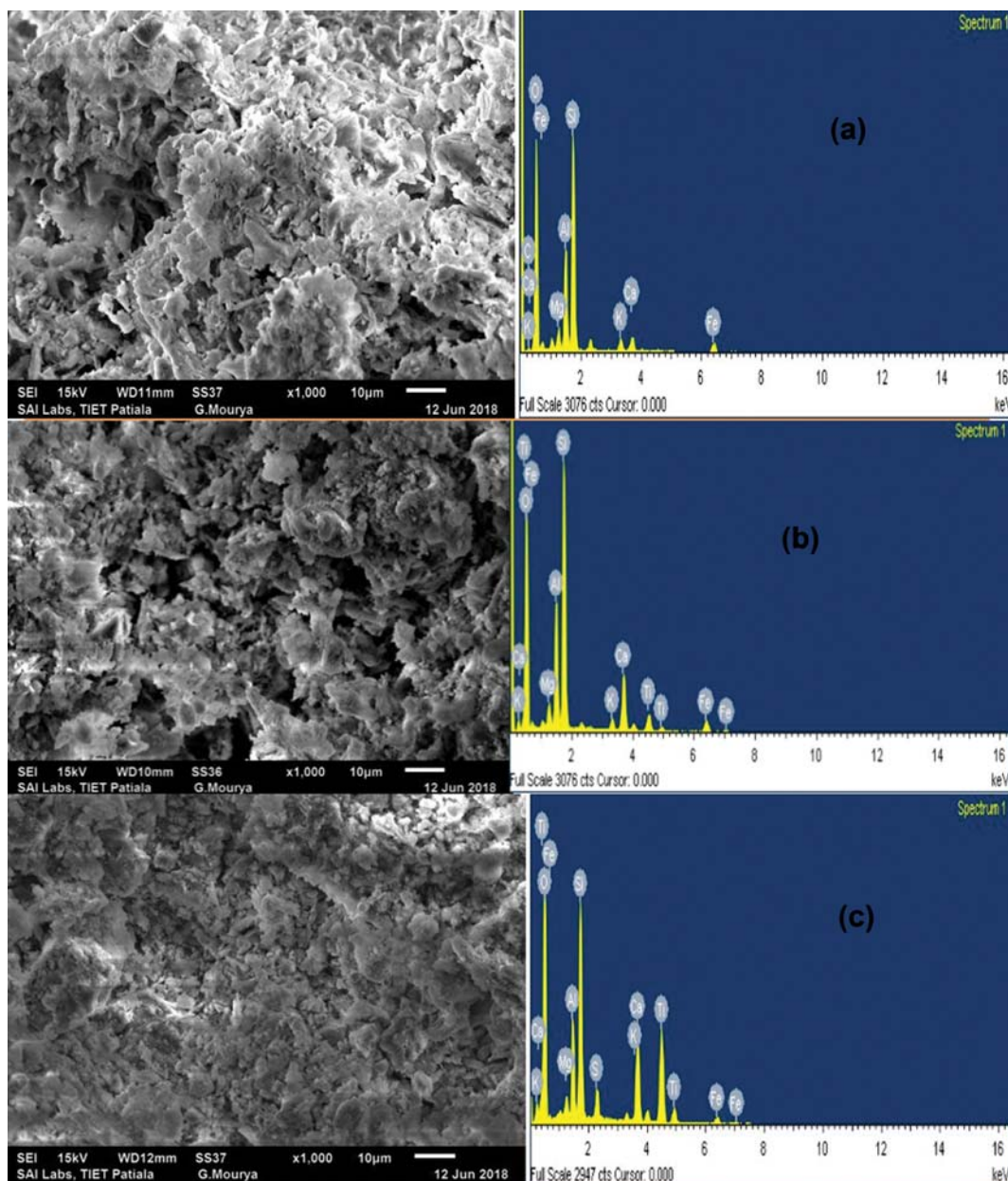


Fig. 6. (a) SEM-EDS of the uncoated beads, (b) SEM-EDS of the freshly coated TiO_2 beads, (c) SEM-EDS of the recycled TiO_2 beads.

uncoated beads Fig. 6(a) confirms the roughness of the beads surface and also the presence of iron at the surface. And for the freshly coated FA+FS (unused) spherical beads, Fig. 6(b) confirms the even coating of TiO_2 over the composite beads and the iron's presence; the recycled beads 6(c), which have been through 35 cycles, shows that the coating of TiO_2 was uniform over the bead surface even after repeated cycles. The presence of Fe, Ti, and O elements was confirmed by observing distinct peaks in EDS as shown in Table S1-S3.

5-4. Mineralization Study

The mineralization of the treated ofloxacin water was carried out by estimating the amount of COD reduced and the generation of nitrate, nitrite and ammonia ions. There was almost 75% reduction in COD after 2 hours. TOC analysis showed 52% of the

removal confirming the mineralization of the ofloxacin (Fig. S3). The nitrogen atoms were converted into the nitrates, ammonium, and nitrites. It was observed that the nitrate ions increased up to 9.8 mg L^{-1} and then started to decrease. After 2 hours 6.5 mg L^{-1} of nitrate ions were observed. This might have been due to the conversion of nitrates to nitrites and ammonium ions. The nitrite ions increased up to $125 \text{ } \mu\text{g L}^{-1}$. The ammonium ions increased up to 1.8 mg L^{-1} in 2 hours [25-27]. The concentration of nitrites and ammonium ions (Fig. S2) increased with time, confirming the mineralization of the ofloxacin, which was further confirmed through the LC-MS analysis.

The mineralization study of ofloxacin was described through LC-MS (Liquid chromatography-Mass spectroscopy) analysis for identification of compounds formed during degradation of ofloxa-

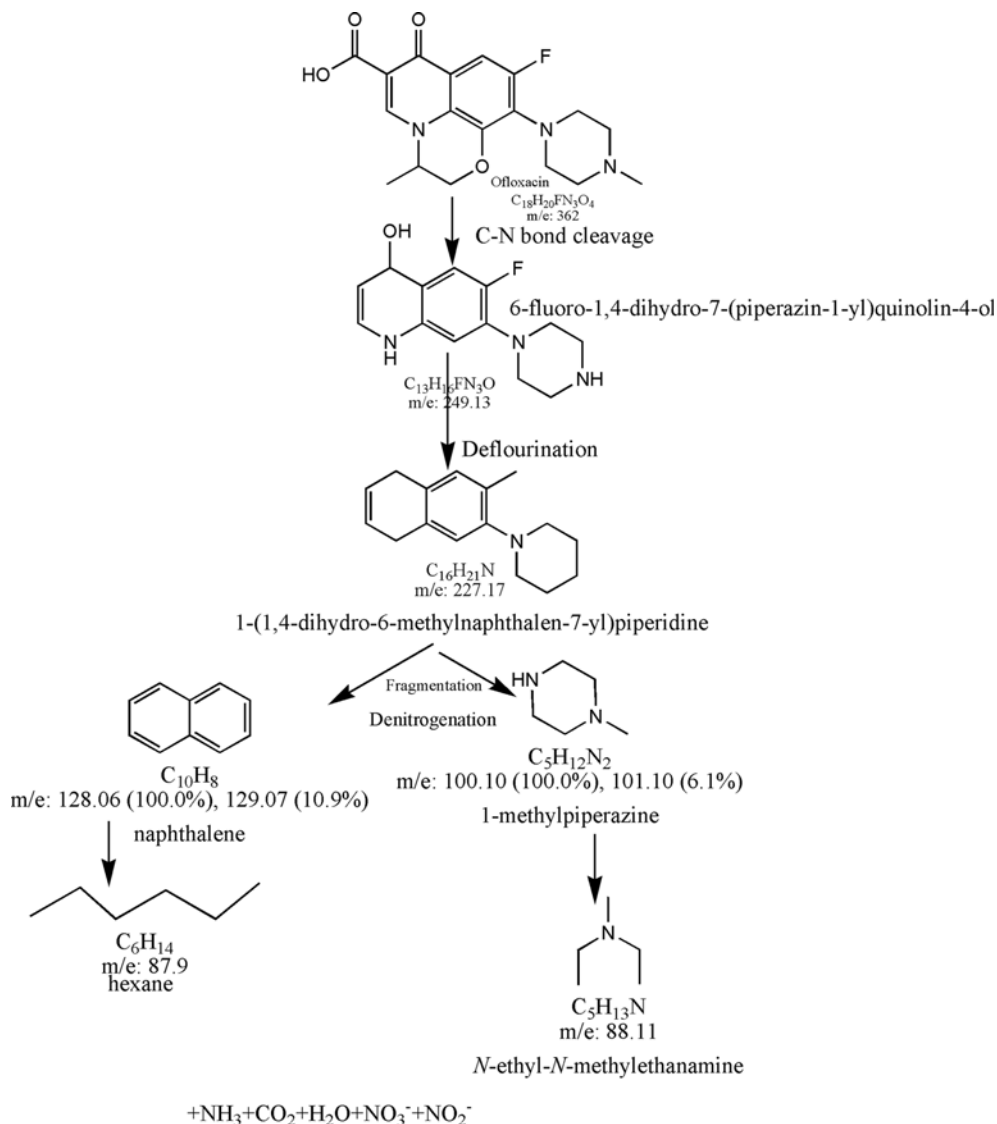


Fig. 7. Tentative pathway for the degradation of ofloxacin.

cin as shown in Fig. 7 along with chromatograms (Fig. S1). The degradation mechanism displayed the formation of a compound 6-fluoro-1,4-dihydro-7-(piperazin-1-yl)quinolin-4-ol by the C-N bond cleavage, which further formed 1-(1,4-dihydro-6-methylnaphthalen-7-yl)piperidine by defluorination, and after that the fragmentation might have led to the formation of two different compounds by denitrogenation, naphthalene and 1-methylpiperazine, which further generated the compounds hexane and N-ethyl-N-methylethanamine, respectively. The former compound by deacetylation formed a benzene ring which further might have reduced into some by-products. The other intermediate inorganic compounds formed included nitrate, nitrite, hydrogen fluoride, ammonia, carbon dioxide, and water.

For toxicity analysis, samples (treated and untreated) were incubated for 24 h, and it was observed that the zone of inhibition did not exist in three sections of the plate (Fig. 8). The absence of a zone of inhibition showed that the pharmaceutical compound had been completely mineralized. It was interpreted that the untreated

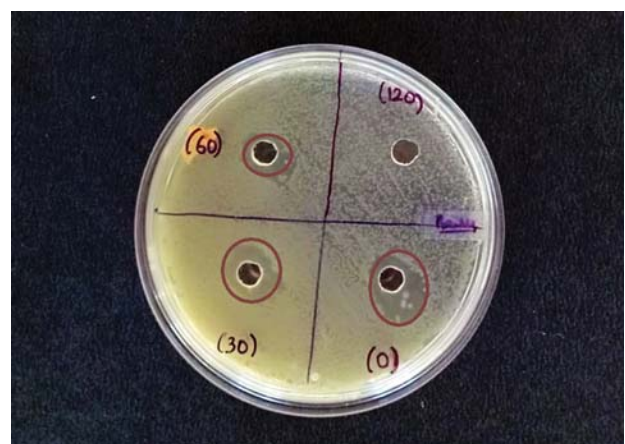


Fig. 8. Toxicity test of ofloxacin showing the zone of inhibition in the section labeled as (0); while the one labeled as (30), (60) and (120) shows the consecutive times of degradation increasing the bacterial growth.

ofloxacin solution was toxic to the bacterial strain as the zone of inhibition was seen but after dual effect degradation [28,29]. Nontoxic to microorganisms, bacteria could survive, which means the drug was completely degraded. The zones for the degradation time showed the reduction in effect of toxicity. The initial diameter of 22 mm at 0 time was reduced to 15 mm and after that to 12 mm at 60 min. After 120 min, complete removal of zone was observed. The zone of inhibition was eliminated and hence, it might be concluded that the treated ofloxacin solution was nontoxic.

CONCLUSION

The study presented the use of composite beads made up of FA, FS (source of iron) and clay for immobilizing TiO₂ used to introduce the in-situ dual effect (photo-Fenton and photocatalysis). The photo-degradation of the pharmaceutical compound ofloxacin was practiced using this dual effect at optimized conditions of pH (3.4), H₂O₂ dose (300 mg L⁻¹), A/V ratio of 0.273 cm² mL⁻¹. The rate of reaction was significantly increased using dual effect as compared to an individual of photo-Fenton and photocatalysis. The overall synergy of this novel dual effect was 51%. The durability studies proved that the composite was quite efficient to be effectively reused even after 35 cycles and that too with the same degradation proficiency as it was seen in the initial reactions. The reused composite retention of the TiO₂ nanoparticles along with leaching of iron was affirmed through different characterization studies like SEM/EDS, UV-DRS, FT-IR. The mineralization of the compound ofloxacin was studied through the intermediates formed during GC-MS analysis and the estimation of nitrate, nitrite, total iron concentrations. The nontoxicity of the treated ofloxacin samples was confirmed by the toxicity assays using *E. coli* grown in nutrient medium. Hence, it was concluded that the dual effect technique was successful in the treatment of pharmaceutical wastewater and has the potential for large scale applications.

SUPPORTING INFORMATION

Additional information as noted in the text. This information is available via the Internet at <http://www.springer.com/chemistry/journal/11814>.

REFERENCES

1. S. P. Pardhe, *Int. Res. J. Pharm.*, **9**, 15 (2018).
2. Q. Sui, X. Cao, S. Lu, W. Zhao, Z. Qiu and G. Yu, *Emerg. Contam.*, **1**, 14 (2015).
3. N. Nassiri Koopaei and M. Abdollahi, *DARU, J. Pharm. Sci.*, **25**, 1 (2017).
4. M. M. Huber, S. Canonica, G. Y. Park and U. Von Gunten, *Environ. Sci. Technol.*, **37**, 1016 (2003).
5. J. Rivera-Utrilla, M. Sánchez-Polo, M. Á. Ferro-García, G. Prados-Joya and R. Ocampo-Pérez, *Chemosphere*, **93**, 1268 (2013).
6. S. Miralles-Cuevas, I. Oller, J. a S. Pérez and S. Malato, *Water Res.*, **64**, 23 (2014).
7. J. Sharma, I. M. Mishra and V. Kumar, *J. Environ. Manage.*, **156**, 266 (2015).
8. S. Talwar, V. Sangal and A. Verma, *J. Photochem. Photobiol. C Photochem.*, **353**, 263 (2018).
9. S. Talwar, V. K. Sangal, A. Verma, P. Kaur and A. Garg, *Arab. J. Sci. Eng.*, **43**, 6191 (2018).
10. A. Verma, A. P. Toor, N. T. Prakash, P. Bansal and V. K. Sangal, *New J. Chem.*, **41**, 6296 (2017).
11. S. Mozia, P. Bro, J. Przepi, B. Tryba and A. W. Morawski, *J. Nanomaterials*, **2012**, 1 (2012).
12. D. Mukherjee, S. Barghi and A. Ray, *Processes*, **2**, 12 (2013).
13. C. Gadiyar, B. Boruah, C. Mascarenhas and V. Shetty, *Int. J. Current. Eng. Technol.*, **84**, 1 (2013).
14. P. Bansal, A. Verma and S. Talwar, *Chem. Eng. J.*, **349**, 838 (2018).
15. F. Tamtam, F. Mercier, B. Le Bot, J. Eurin, Q. Tuc Dinh, M. Clément and M. Chevreuil, *Sci. Total Environ.*, **393**, 84 (2008).
16. L. Gao, Y. Shi, W. Li, H. Niu, J. Liu and Y. Cai, *Chemosphere*, **86**, 665 (2012).
17. A. Verma, N. T. Prakash and A. P. Toor, *Chemosphere*, **109**, 7 (2014).
18. APHA, *Am. Public Heal. Assoc. Washington*, DC, USA (2012).
19. A. D. Bokare and W. Choi, *J. Hazard. Mater.*, **275**, 121 (2014).
20. A. P. Toor, A. Verma, C. K. Jotshi, P. K. Bajpai and V. Singh, *Dyes Pigm.*, **68**, 53 (2006).
21. P. Bansal and A. Verma, *Mater. Des.*, **125**, 135 (2017).
22. P. Bansal and A. Verma, *J. Photochem. Photobiol. A Chem.*, **342**, 131 (2017).
23. D. Kannaiyan, S. T. Kochuveedu, Y. H. Jang, Y. J. Jang, J. Y. Lee, J. Lee, J. Kim and D. H. Kim, *Polymers (Basel)*, **2**, 490 (2010).
24. S. Dagher, A. Soliman, A. Ziout, N. Tit, A. Hilal-Alnaqbi, S. Khashan, F. Alnaimat and J. A. Qudeiri, *Mater. Res. Express.*, **5**, 1 (2018).
25. APHA, AWWA, and WEF, *Stand. Methods Exam. Water Wastewater* (2005).
26. APHA/WEF/AWWA, *Stand. Methods Exam. Water Wastewater* (2018).
27. APHA, in *Stand. Methods Exam. Water Wastewater* (2012).
28. A. Mirzaei, Z. Chen, F. Haghighat and L. Yerushalmi, *Appl. Catal. B Environ.*, **242**, 337 (2019).
29. G. Sági, A. Bezsényi, K. Kovács, S. Klátyik, B. Darvas, A. Székács, C. Mohácsi-Farkas, E. Takács and L. Wojnárovits, *Sci. Total Environ.*, **622-623**, 1009 (2018).